CAMPUS ENERGY MODEL: USING A SEMI-AUTOMATED WORKFLOW TO BUILD SPATIALLY RESOLVED CAMPUS BUILDING ENERGY MODELS FOR CLIMATE CHANGE AND NET-ZERO SCENARIO EVALUATION

Thomas Suesser, Timur Dogan
tds78@cornell.edu, tkdogan@cornell.edu
Environmental Systems Lab, Cornell, Ithaca, New York, USA

Abstract

To meet carbon reduction goals, municipalities, universities, and other large organizations need reliable and adaptable models that provide detailed building performance metrics to efficiently manage future energy demand. At the urban scale, models are often restricted by access to usage and geometry data and can only accurately predict aggregate energy demand based on historic data or statistical models. This paper seeks to present a novel workflow that uses institutional GIS datasets to produce calibrated multi-zone energy models for future scenario assessment and to inform building retrofitting options. The authors hope that the introduced workflow leads to a wider adoption of the involved tools to support the environmental strategies of others.

Introduction

In recent years, climate change and rapid urbanization have each become inevitabilities. By 2050, two-thirds of the world's population will live in urban areas (United Nations, Department of Economic and Social Affairs, and Population Division 2012), the same year by which every nation on earth pledged to obtain zero carbon emissions in the 2016 Paris Climate Agreement (Chan and Eddy 2015). At the same time, traditional association of cities as dirty pollution centers have also given way to the theory that high density urban centers hold the key to feasible sustainable development. Thus, the need for sustainable development in urban areas continues to increase. Since it is usually undesirable to simply demolish and rebuild in dense urban areas, especially in developed countries, building retrofitting on massive scales must occur to reach carbon reduction targets set by nations, states, and municipalities. Thus, the ability to analyze the energy use of existing buildings in climate change and retrofitting scenarios has become increasingly important.

In order to achieve reliable predictions of future energy use, it is necessary to first develop detailed models representative of the existing building geometry which can be simplified and integrated into energy simulations. Advances in the field of building simulation have made it easier to integrate building geometry (Dogan and Reinhart 2017), material definitions, load profiles, and other properties (Cerezo, Dogan, and Reinhart 2014). However, processes that yield detailed, accurate, and usable geometry are often still "error prone and tedious" (Schlueter and Thesseling 2009). A streamlined, semi-automated process of integration of building geometry is yet to be developed. This process must also allow for the revision of physical building characteristics in order to simulate and inform retrofitting scenarios. For the same reason, this model must also validated against historical energy usage data. One must be able to understand the effect of multiple parameters on the data, not simply "fudging" the model parameters in order to achieve calibration with existing data, but follow a documented mathematical process. Problems with such a technique have been documented, such as their inaccuracy and time and computational intensiveness (Coakley, Raftery, and Keane 2014). In energy modeling during the building design phase, more emphasis can be placed on the final results of the simulation. However, in modeling existing buildings it is necessary to place greater emphasis on behavior in time and thus to measure calibration success based on both aggregate demand and hourly demand.

An accurate and comprehensive modeling tool is needed in order to obtain this degree of resolution. Energy-Plus simulation has been touted for its ability to simulate multi-zone airflow and integrate extensive HVAC systems, making it one of the most popular simulation programs in the field of building simulation (Coakley, Raftery, and Keane 2014; Nguyen, Reiter, and Rigo 2014).

Current building simulation efforts are often beholden to their access to both geometry and energy data, placing limitations on calibration accuracy. The author's home institution provides an ideal case study for a variety of factors including the good availability of GIS, building, and measured high-resolution energy consumption data in hourly resolution. Even with reliable usage data, success is usually measured by error in aggregated yearly or monthly measured vs. simulated energy use (Reinhart and Cerezo Davila 2016).

This paper seeks to calibrate hourly demand curves while maintaining high geometric resolution in the models so that retrofitting recommendations can be given. Producing geometrically detailed energy models usually is time and cost-prohibitive as it involves manually splitting buildings into multiple zones and providing zone descriptions for the resulting enclosed volumes. This paper presents an automated workflow that utilizes

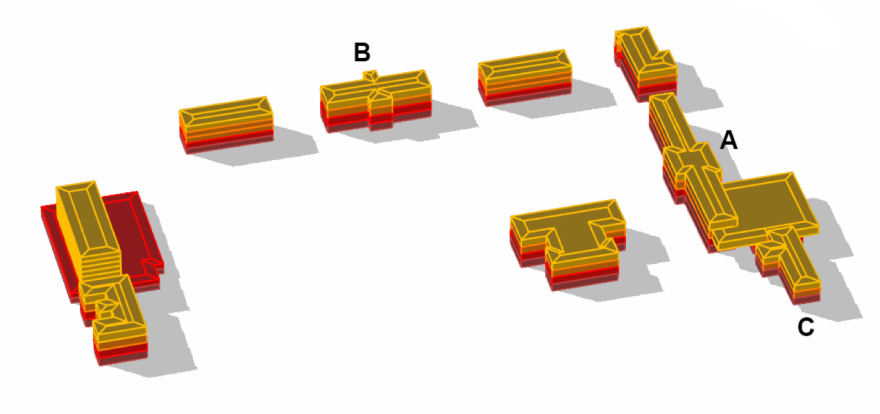

Figure 1: Building geometries colored by floor type and thermal zone divisions

institutional GIS data-sets to generate multi-zone building energy models for scenario evaluation and planning aid. Therefore, a variety of different workflows ranging from GIS parsing, geometric computing and modeling, data matching, energy model setup, simulation and optimization tools need to be brought together. Coupling these complex systems into one easily manipulated and reliable model remains challenging and hence this paper seeks to present a feasible and efficient workflow to create calibrated models of existing buildings on a university campus scale. The paper implements several automata to generate relevant input data and seamlessly connects a set of existing tools. The workflow aims to produce models that are accurate and detailed enough to be used to inform design and planning decisions including future retrofitting projects and climate change scenarios in pursuance of the institutional carbon neutrality targets. or this study three buildings have been analyzed. Other campus buildings will follow in subsequent studies.

Simulation

General Approach

The process of specifying building properties to achieve calibration was carried out in three main parts. First, the building geometries were generated from GIS shape files and split into thermal zones for each floor. Second, building construction, usage schedules, load profiles, and ventilation characteristics were specified for each zone. Lastly, an automated simulation workflow using EnergyPlus (Crawley et al. 2000) and the Archsim plug-in (Dogan 2016) for Rhino (Robert McNeel & Associates 2016b) and Grasshopper (Robert McNeel & Associates 2016a) assigned these parameters to the zones as specified using the Goat optimization solver component with local, linear approximations (COBYLA) (Flory 2016) and ran an simulations based on historical weather data measured with an weather station located on the rooftop of one of the analyzed buildings.

The geometries were specified from institutional GIS data and constructed using an automated process. GIS data was loaded into Rhinoceros and the building footprint polygons were parsed from the GIS data. A custom script using a modified Douglas-Peuker algorithm was used to automatically remove redundant points and to simplify overly fine discretization of curvature to keep the overall geometric complexity manageable for BEM tools. Special attention was given to corner points if they are adjacent to a neighboring building. Such points were locked in place and were not subject to simplification. Since adjacency detection in later steps relies on congruent edges, overlapping lines were split until congruent. Further, the footprint area is a relevant property. In this case, geometric footprint area of the shapefile did not always match more accurate data entries from institutional sources that specified either footprint or overall floor area. Iterative offsetting was used to manipulate the original shape to match geometric and data derived foot print area.

The processed footprints were then automatically broken into thermal zones according to the recommendations given in ASHRAE 90.1 Appendix G (ASHRAE 2013) using straight skeleton based automatic zoning. (Dogan, Reinhart, and Michalatos 2016). The zones were then extruded to form thermal blocks for each floor of the building. Figure 1 shows the buildings and thermal zone geometry. The thermal zones were then paired with data templates that describe materiality, loads and conditioning settings of each zone. Templates are specific to each building and include detailed zone descriptions for core and perimeter regions located in the basement, ground, intermediate and roof floors. For the template assignment process, zone adjacencies and overall location in the building such as in the basement, ground level/first floor, in-between floor or roof zones are detected automatically using a custom script that traverses the zone and face graph.

An Excel spreadsheet was used to gather and compile the input parameter templates for each zone and then dynamically linked to the energy model generation workflow in Rhino/Grasshopper. The spreadsheet format for model input data aggregation facilitated sharing model assumptions with others such as facility management as well as updating batches of input data for multiple buildings. Further, entries could be updated with a tablet or smartphone during field assessment.

Window to wall ratios were measured from photographs taken of building façades and constructions as shown in Figure 2. The glazing system specification as well as the

constructions for roof, façade and basement were specified from field assessment. When construction assemblies where unknown, visual inspection and heat flux measurements using the GSKIN U-Value Kit were performed. Figure 3 shows a long-term study of a wall in Building A. U-Values at night time where averaged and used as basis to estimate materials and thicknesses of a construction. Figures 4-7 show the most important constructions used in this study. Table1 provides the U-Values. In addition to the contextual shading from GIS based building volumes, other significant obstructions such as large trees or overhangs were added to the model based on field assessment observations.

Figure 2: Building A façade shown with superimposed polygons for window to wall ratio calculation

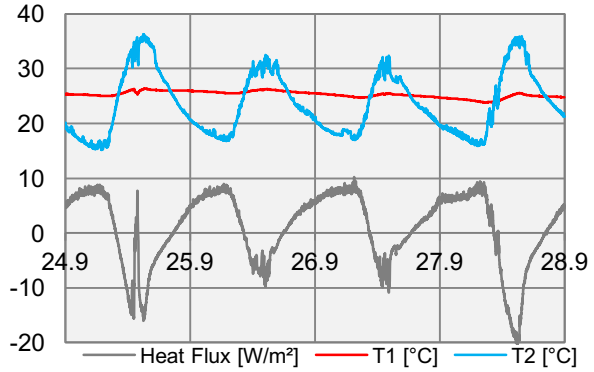

Figure 3: Heat flux measurement to determine wall U-Values for Building A

Electrical equipment usage schedules were extracted from metered electricity demand at building level. Occupancy schedules were based on architectural norm assumptions (Merkblatt 2006). However, when the electricity demand indicated regularly occurring peaks in the morning and lows in the evening - the start and end time of the occupancy schedules were adjusted accordingly.

Once all inputs were gathered, a Grasshopper based workflow using Archsim and Energy Plus was used to batch simulate all models. The models, along with a custom weather file constructed from historical weather data measured on a neighboring building, were inputted into two separate EnergyPlus simulations for heating and cooling load calibration. One simulation ran for a week in September and the other for a two-week period in December.

The rather short calibration periods were selected due to limited data availability of both the metered energy demand and weather data. However, the periods are somewhat representative since they cover the warmer and more humid season in the summer as well as the winter period with both an occupied week as well as the winter holiday season.

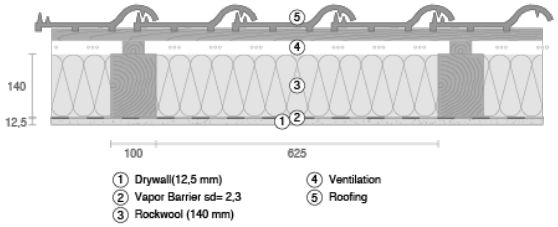

Figure 4: Building A and B roof construction.

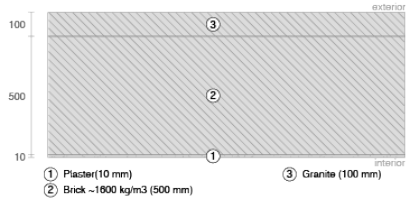

Figure 5: Building A and B façade construction

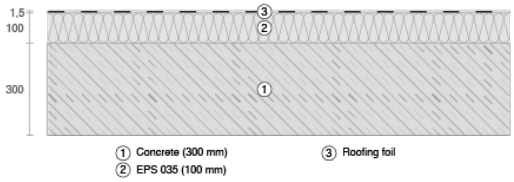

Figure 6: Building C roof construction

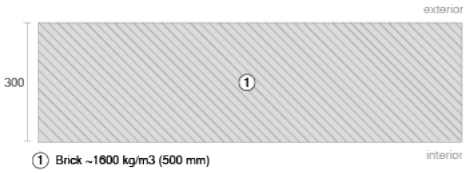

Figure 7: Building C facade construction

Table 1: Building properties.

Building Name	**Bldg A**	**Bldg B**	**Bldg C**
Floor Area (m^2)	6605	4298	2514
Windows	Single	Single	Single
Facade (W/m^2K)	1.05	1.05	1.85
Roof (W/m^2K)	0.34	0.34	3.2
Power density (W/m^2)	9.33	10.82	46.30
People (p/m^2)	0.199	0.072	0.200
Infiltration (ACH)	0.809	1.20	0.738
Internal Mass ratio (m^2/zone area)	0.150	0.028	0.191

Calibration

The goal of the calibration step is to validate the produced models so that they accurately predict existing conditions. The locally measured historic weather data and metered demand curves were used for this. Calibration success was measured by comparing simulated cooling and heating energy with measured usage for the same periods in September and December 2015, respectively. A hybrid function of the root mean squared error of the hourly heating and cooling series and the percent error of the aggregate heating and cooling demand, as shown in Equations 1 and 2, was used as fitness function. The overall percentage difference for the total heating and cooling load was weighted slightly higher as the accuracy in hourly resolution.

$$E_T = 0.4 * (RMSE_H + RMSE_C) + 0.6 * Diff \quad (1)$$

$$Diff = \frac{(Heat_{mes} - Heat_{sim})}{Heat_{mes}} + \frac{(Cool_{mes} - Cool_{sim})}{Cool_{mes}} \quad (2)$$

The most challenging part of the calibration step is to identify parameters that are certain and reliable and those that are uncertain. The authors could specify some parameters with exact certainty or near certainty, such as building constructions, internal mass exposed surface area ratio, window to wall ratios, window glazing materials, contextual shading and shading systems as well as electrical equipment usage. Other parameters were less obvious, hard to measure on site and therefore uncertain. These could be specified within a reasonable range, but no further. Sensitivity analysis was then used to narrow down the focus of the calibration. The authors could identify two parameters – infiltration rate and people density - that had significant impact on the simulation results. Based on the authors' experience, reasonable ranges have been assumed to be 0.1 to 3 (ACH), 0.02 to 0.2 (p/m^2) for infiltration rate, people density. Less influential parameters were set to the median value within the range that was deemed realistic. Linear approximation (COBYLA) was used to optimize the most influential parameters over a reasonable range. This minimized error as specified in Formula 1 and 2. Figures 8 - 11 show calibrated usage curves in hourly resolution for both heating and cooling demand for buildings A - C. Table 2 juxtaposes the simulated and metered total heating and cooling demand for the calibration periods based on which the percentage errors ranging from 7% to -15.4% in Table 3 are computed. Metered heating data for Building C and cooling data for Building B were not available.

The calibration did yield similar infiltration rates (given in Table 1). This is plausible given that all three buildings have similar size, materiality and a relatively poor construction standard. The estimated people density is however very significantly higher in Building A and C compared to the estimate in Building B. A and C are both used by the Architecture School and densely populated and usually used around the clock.

Table 2: Total heating and cooling demand metered and simulated for the summer (09/23/15-09/30/15) and winder (12/17/15-12/31/15) calibration periods

	Bldg A	**Bldg B**	**Bldg C**
Metered Heating Total (kWh/m^2)	17.795749	14.163468	N/A
Simulated Heating Total (kWh/m^2)	16.50065	14.155996	N/A
Metered Cooling Total (kWh/m^2)	2.415758	N/A	2.71354
Simulated Cooling Total (kWh/m^2)	2.122319	N/A	2.296996

Table 3: Percentage error in predicted heating and cooling demand compared to metered data for the summer (09/23/15-09/30/15) and winder (12/17/15-12/31/15) calibration periods

	Bldg A	**Bldg B**	**Bldg C**
Total heating percentage error	*7%*	*0.053%*	*N/A*
Total cooling percentage error	*-7.3%*	*N/A*	*-15.4%*

Scenario Assessment

With three buildings calibrated to a satisfactory accuracy level in temporal thermal behavior and absolute demand, the models were then used to quantify energy impacts of climate change predictions and various retrofitting scenario. Simulations for one entire year using a Typical Meteorological Year (TMY) weather file from the nearest airport were performed.

Climate Change

As the world's climate continues to change and large entities like universities aim for sustainability and carbon neutrality in the long term. To achieve such a goal, it is important to predict how buildings will respond to changing weather patterns in the future. Using the CCWorldWeather Gen tool by Jentsch, Bahaj, and James (2008), climate files for the years 2020, 2050, and 2080 were generated by morphing a TMY from the nearest airport. Each building is then analyzed in current and future conditions.

Figures 10 – 12 show how the three buildings respond to changing climate. As seen in Figure 10, with no change in any parameters besides climate, Building A experienced very little overall change in energy demand. A 4% reduction in total demand by 2080 can be observed. However, as the climate warms the model predicts that a greater share of the energy demand will fall on cooling loads. In 2015 cooling accounted for 8.8% of the energy demand (the sum of heating, cooling, and electrical equipment) for Building A. By 2080, this number has grown to 23.8%.

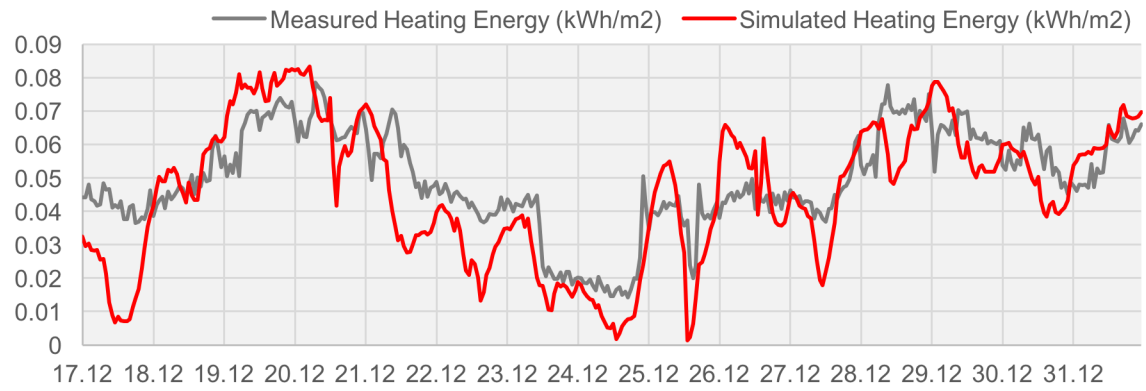

Figure 8: Building A measured vs. simulated hourly heating energy

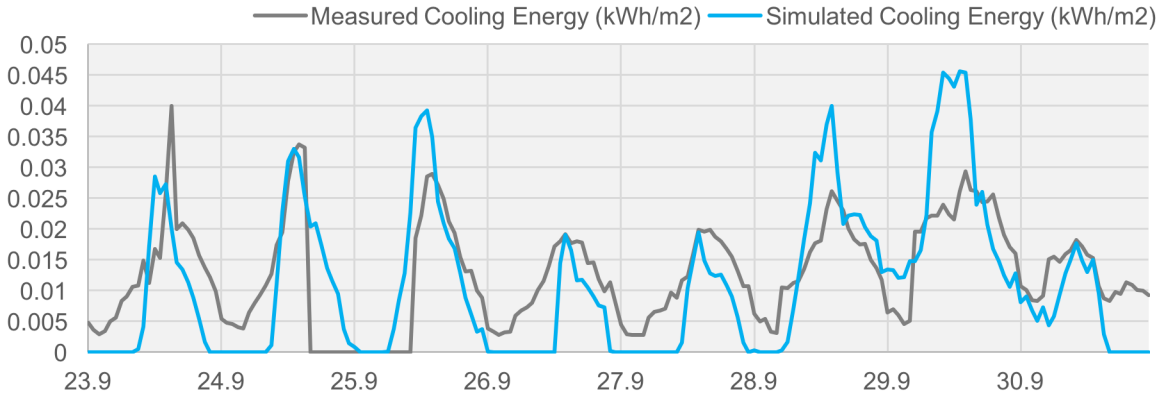

Figure 9: Building A measured vs. simulated hourly cooling energy

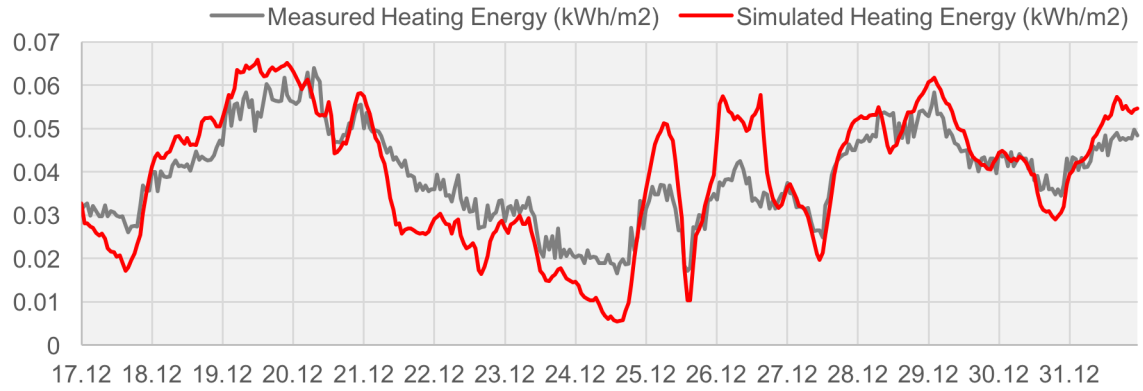

Figure 10: Building B measured vs. simulated hourly heating energy

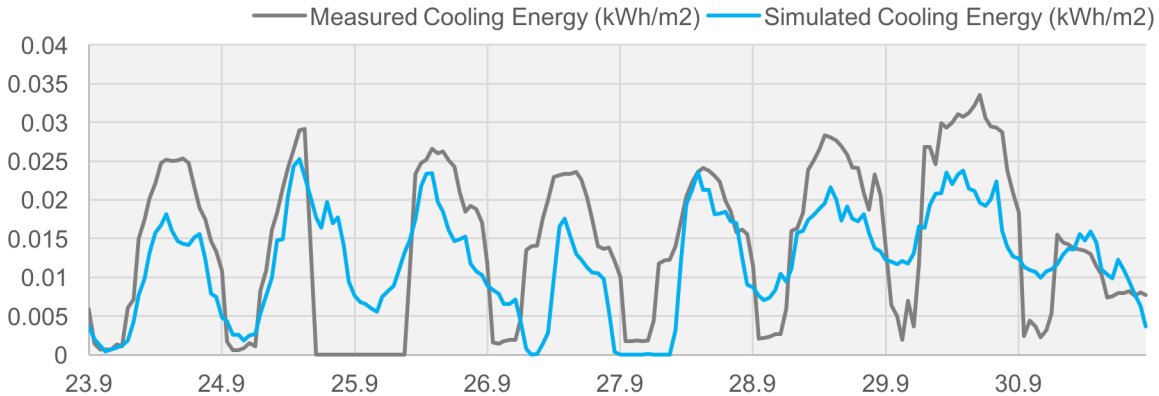

Figure 11: Building C measured vs. simulated hourly cooling energy

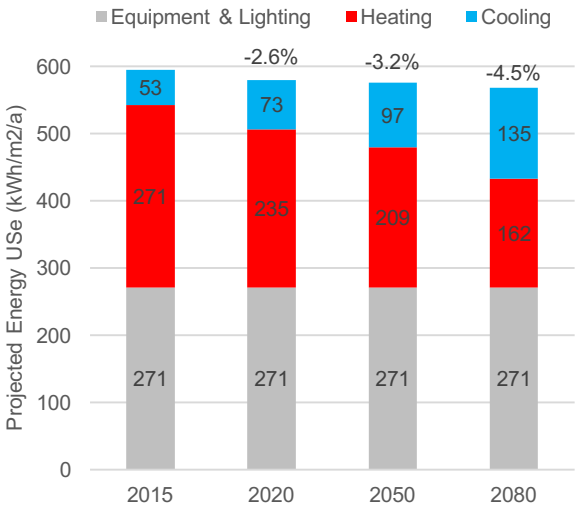

Figure 10: Building A predicted energy demand based on climate change.

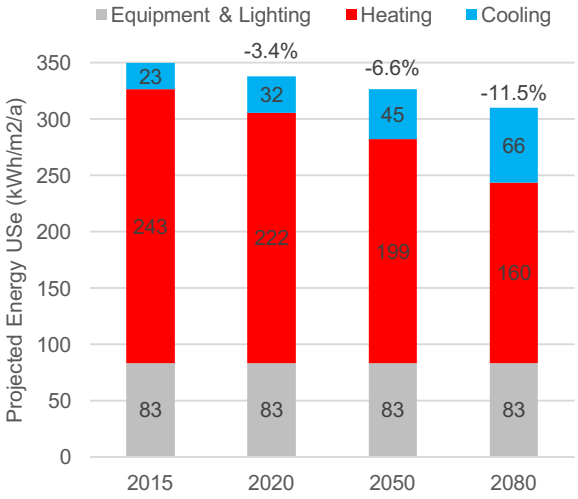

Figure 11: Building B climate change response

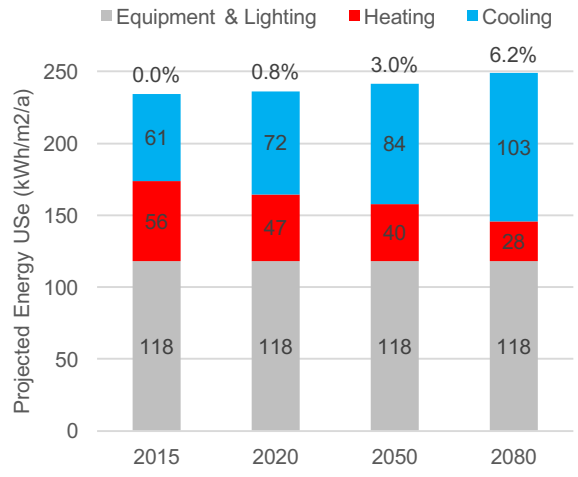

Figure 12: Building C climate change response

This represents an increase by 386%. This shift towards cooling energy will place a signifiantly higher burden on the cooling infrastructure of the authors' home institution. This trend continues for Building B and Building C, as seen in Figures 11 and 12, with cooling's share of total energy demand jumping from for 6.6% to 21.3% and 25.8% to 41.4% from 2015 to 2080, respectively. However, neither Building B's nor Building C's total energy demand remains constant. In the case Building B, total energy demand falls by 11.5% by 2080, while Building C's total energy demand grows by 6.2%.

While heating demand shrinks significantly in all buildings, it remains the dominant load in both Buildings A and B. This adds to the justification of investment in sustainable heating sources even in the face of gradually rising temperatures.

The degree of variance in results between the buildings reveals the need for separate building simulations, as each building's unique characteristics make it respond differently to climate change.

Electrical Equipment Demand Reduction

One parameter likely to change with advances in technology is electrical equipment energy demand. In this model, lighting is grouped into electrical equipment, as the institution's facilities management does not meter electricity separated by end-use. Changing building light bulbs from incandescent to compact fluorescent lights (CFL) or LED bulbs can save a tremendous amount of energy, and is a practice gradually being adopted worldwide. In large academic buildings, however, upgrading lightbulbs is only one aspect of potential electrical equipment energy demand reduction. Switching office computers from desktops with separate monitors to more efficient laptops is one such measure. A typical desktop computer runs at between 80W and 250W, whereas laptops can be charged around 45W.

Equipment energy demand also adds significant heat to buildings. In the following study, the authors assume that electrical equipment energy demand will decrease by 10% by 2020, 25% by 2050, and 50% by 2080. These scenarios are analyzed for each building in conjunction with climate change. The results are given in Figures 13, 14, and 15.

As expected, reducing electrical equipment energy has a significant impact on the total building energy demand and therefore is beneficial for any institution's bottom line and carbon neutrality efforts. Further, the reduction in electricity consumption lessens the increase in summer cooling loads due to climate change. The reduction in internal gains, however, does not lead to an increase in heating demand due to the rising exterior temperatures. In Building C the reduction stabilizes the heating and cooling loads. While these results are somewhat expected, quantifying the effect is still valuable. For example, this information could be used for targeted plug load reduction in buildings with low capacity heating or cooling systems to ensure a longer building lifetime if system upgrades are difficult or too expensive.

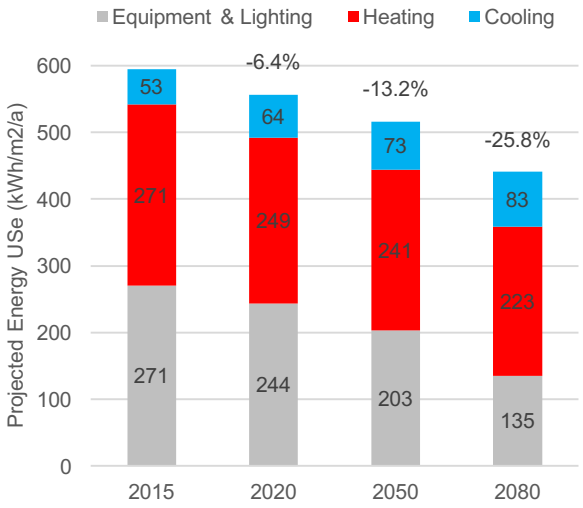

Figure 13: Building A site-electrical reduction response

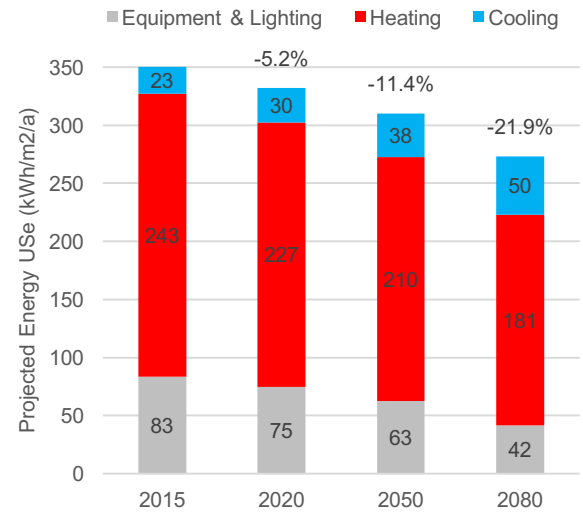

Figure 14: Building B site-electrical reduction response

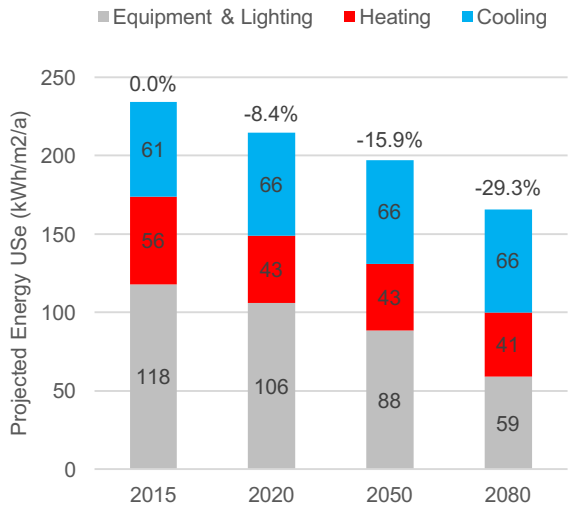

Figure 15: Building C site-electrical reduction response

Window Retrofitting

Another investment that can save significant amounts of energy with limited invasion of the existing building is window retrofitting. All three of the buildings discussed in this paper were built over one hundred years ago and contain clear, single pane casement windows. These trap very little heat, and cause unwanted infiltration at their numerous seems and joints, making them highly inefficient during both warm and cool months.

For this study three retrofitting options are analyzed. The first, referred hereafter as DoublePaneLoE2 is a double paned window with a low emissivity coating inner surface of the outer pane. The second, referred to hereafter as DoublePaneLoE3, is a double paned window with the low emissivity coating on the interior surface. The third, referred to hereafter as TriplePaneLoE, is a triple pane window with the low emissivity coating on layers e2 and e5, which are the interior of the outermost pane and the outermost surface of the innermost pane. Table 2 details the thermal properties of each of these windows, as well as the existing single clear-paned windows, where Tvis is the Visible Light Transmission factor, Uval is the U-Value, and Shgf is the Solar Heat Gain Coefficient.

Window Type	Tvis	Uval	Shgf
SinglePaneClr	0.913	5.894	0.905
DoublePaneLoE2	0.444	1.493	0.373
DoublePaneLoE3	0.769	1.507	0.649
TriplePaneLoE	0.661	0.785	0.764

Table 2: Window Properties

Heating and cooling energy demand for each building was calculated for each window option in current and future climate scenarios. The metered electrical equipment energy was left unchanged but omitted for reporting as the retrofits have no effect on this value (no daylight simulations for dimming of electric lighting was conducted). The results are given as bar charts showing overall energy impact from 2015 to 2080 (Figure 16-18) and as linearly interpolated time series (Figures 19-21).

While the results of the climate change and electrical equipment energy demand reduction scenarios differ for each building, all three buildings have similar responses to the window retrofitting scenarios. The introduction of a double pane glass leads to a significant drop in cooling and heating energy consumption in all three buildings. Building A and B yield a 33% and 55% reduction respectively, whereas Building C offers only a 17.2% savings potential. The triple pane option does not provide significant benefits over the double pane glass despite its better U-Value. This is a result of the remaining poor façade and roof constructions. Thus, investment should be directed most immediately to Building B for the greatest return on investment. Still all three buildings would achieve significant energy demand reductions if all windows were replaced by the double pane windows with low SHGCs.

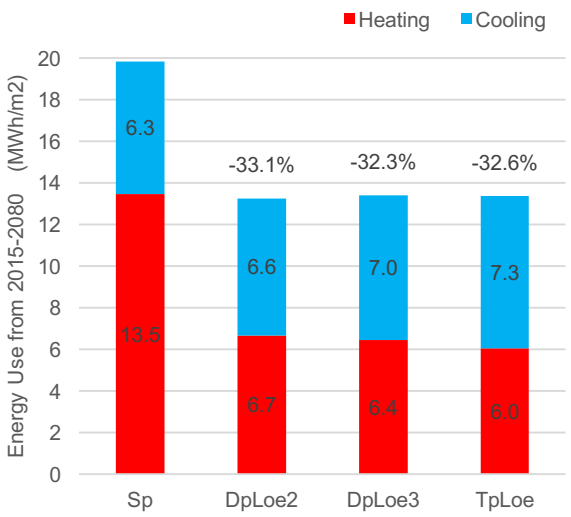

Figure 16: Energy impact of window retrofitting options for Building A from 2015-2080.

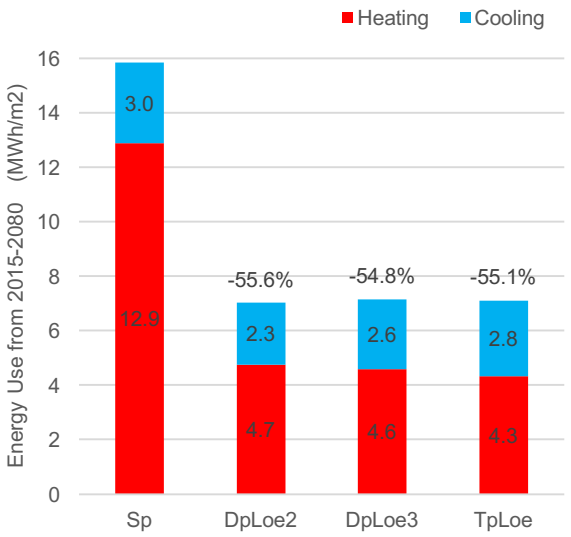

Figure 17: Current conditions and retrofitting options for Building B in future climate scenarios.

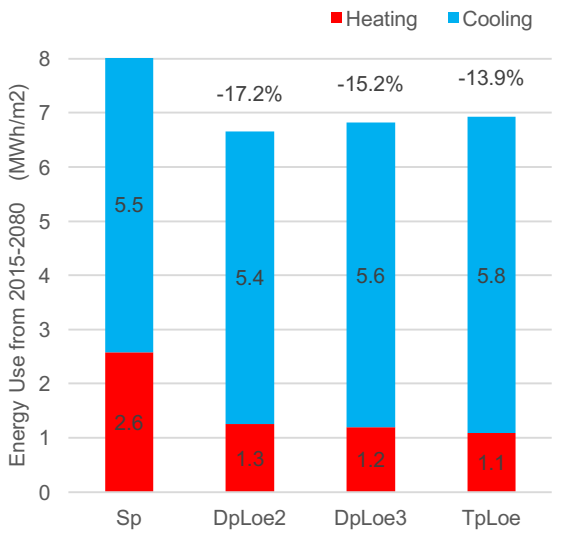

Figure 18: Current conditions and retrofitting options for Building C in future climate scenarios.

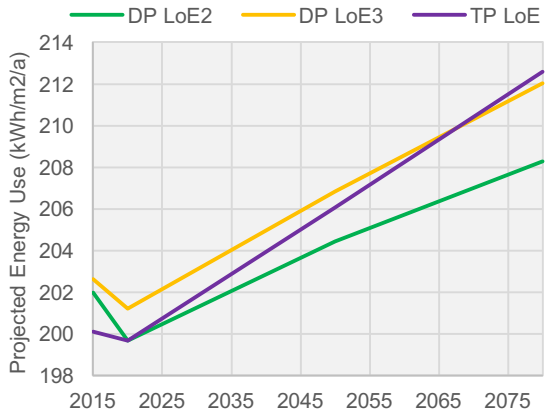

Figure 19: Performance of window retrofitting options for Building A over time.

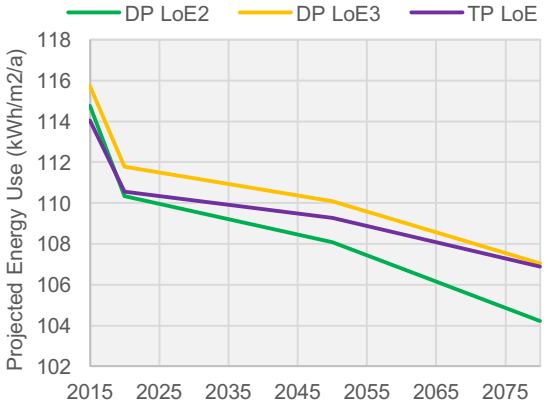

Figure 20: Performance of window Retrofitting Options for Building B in future climate scenarios

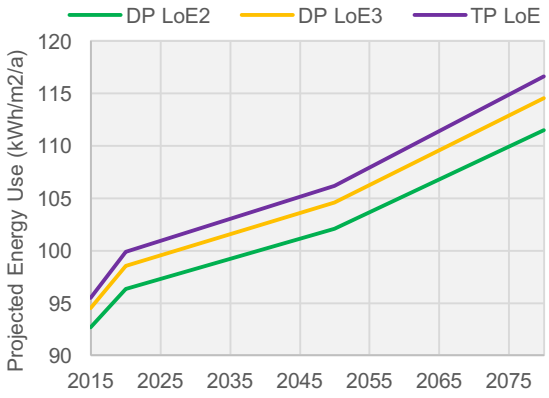

Figure 21: Performance of window Retrofitting Options for Building C in future climate scenarios

Figures 19 - 21, highlight the change in performance of each window type with climate change.

This result demonstrates the importance of analyzing retrofitting options with climate change factored into a building energy model. However, at current estimates of the quickness and severity of climate change, weather morphing should be used to run future scenarios, as the performance of certain designs may vary with these

climate shifts, prompting forward thinking designers and engineers to make different design decisions.

Conclusion

This paper has demonstrated a feasible and efficient workflow to create calibrated models of existing buildings that are accurate and detailed enough to be used to inform decisions for building retrofitting in various climate scenarios in pursuance of carbon neutrality targets. An automated process to generate building energy models from institutional datasets has been outlined.

The usefulness of such the presented workflow was demonstrated in several scenario evaluations including climate change, electrical equipment energy demand reduction and window retrofitting. The information obtained can be used to select between options, to inform policy and for targeted investment. This process of building simulation and its results have underscored the importance of conducting analyses of separate buildings even at campus or neighborhood scale. While most of the results support the intuition of an experienced energy modeler, there is great value in the ability to quantify energy impacts at high spatial and temporal resolution. Unless sufficient funds are available for large scale overhauls, efforts in pursuit of carbon neutrality, are most likely to be carried out in small steps. To maximize the impact of these gradual investments, fast methods for the generation and calibration of individual building energy models are needed. Hence, it is the authors' intention to conduct future studies of this type on more campus buildings and to see the results of these studies used to inform real change in pursuit of the institution's carbon neutrality goal.

Acknowledgements

The authors would like to thank the Cornell University David R. Atkinson Center for a Sustainable Future for funding this research

References

ASHRAE. 2013. "90.1 Energy Standard for Buildings Except Low-Rise Residential Buildings." In *ASHRAE*.

Cerezo, Carlos, Timur Dogan, and Christoph Reinhart. 2014. "Towards Standardized Building Properties Template Files for Early Design Energy Model Generation." In *Proceedings of the ASHRAE/IBPSA-USA Building Simulation Conference*, 25–32.

Chan, Coral Davenport, Justin Gillis, Sewell, and Melissa Eddy. 2015. "Inside the Paris Climate Deal." *The New York Times*, December 12. http://www.nytimes.com/interactive/2015/12/12/world/paris-climate-change-deal-explainer.html.

Coakley, Daniel, Paul Raftery, and Marcus Keane. 2014. "A Review of Methods to Match Building Energy Simulation Models to Measured Data." *Renewable and Sustainable Energy Reviews* 37 (September): 123–41. doi:10.1016/j.rser.2014.05.007.

Crawley, Drury B, Curtis O Pedersen, Linda K Lawrie, and Frederick C Winkelmann. 2000. "EnergyPlus: Energy Simulation Program." *ASHRAE Journal* 42 (4): 49.

Dogan, Timur. 2016. *Archsim*. Accessed May 15. www.archsim.com.

Dogan, Timur, and Christoph Reinhart. 2017. "Shoeboxer: An Algorithm for Abstracted Rapid Multi-Zone Urban Building Energy Model Generation and Simulation." *Energy and Buildings* 140: 140–153.

Dogan, Timur, Christoph Reinhart, and Panagiotis Michalatos. 2016. "Autozoner: An Algorithm for Automatic Thermal Zoning of Buildings with Unknown Interior Space Definitions." *Journal of Building Performance Simulation* 9 (2): 176–189.

Flory, Simon. 2016. *Goat Optimization Add-on Solver*. Accessed November 22. http://www.grasshopper3d.com/group/goat.

Jentsch, Mark F., AbuBakr S. Bahaj, and Patrick A. B. James. 2008. "Climate Change Future Proofing of buildings—Generation and Assessment of Building Simulation Weather Files." *Energy and Buildings* 40 (12): 2148–68. doi:10.1016/j.enbuild.2008.06.005.

Merkblatt, SIA. 2006. "2024: Standard-Nutzungsbedingungen Für Die Energie-Und Gebäudetechnik." *Zürich: Swiss Society of Engineers and Architects*.

Nguyen, Anh-Tuan, Sigrid Reiter, and Philippe Rigo. 2014. "A Review on Simulation-Based Optimization Methods Applied to Building Performance Analysis." *Applied Energy* 113 (January): 1043–58. doi:10.1016/j.apenergy.2013.08.061.

Reinhart, Christoph F., and Carlos Cerezo Davila. 2016. "Urban Building Energy Modeling – A Review of a Nascent Field." *Building and Environment* 97 (February): 196–202. doi:10.1016/j.buildenv.2015.12.001.

Robert McNeel & Associates. 2016a. *Grasshopper*. http://www.grasshopper3d.com/.

———. 2016b. *Rhinoceros* (version 5). https://www.rhino3d.com/.

Schlueter, Arno, and Frank Thesseling. 2009. "Building Information Model Based Energy/Exergy Performance Assessment in Early Design Stages." *Automation in Construction* 18 (2): 153–63. doi:10.1016/j.autcon.2008.07.003.

United Nations, Department of Economic and Social Affairs, and Population Division. 2014. *World Urbanization Prospects: The 2014 Revision : Highlights*.